Supplementary Information

Cyclophilin A promotes cell migration via the Abl-Crk signaling pathway

Tamjeed Saleh[1,2,3], Wojciech Jankowski[2,3], Ganapathy Sriram[4], Paolo Rossi[1,2,3], Shreyas Shah[3], Ki-Bum Lee[3], Lissette Alicia Cruz[5], Alexis J. Rodriguez[5], Raymond B. Birge[4] & Charalampos G. Kalodimos[1,2,3*]

[1]Department of Biochemistry, Molecular Biology & Biophysics, University of Minnesota, Minneapolis, MN 55455.

[2]Center for Integrative Proteomics Research and [3]Department of Chemistry & Chemical Biology, Rutgers University, Piscataway, NJ 08854.

[4]Department of Biochemistry & Molecular Biology, Rutgers Biomedical and Health Sciences, Newark, NJ 07103.

[5]Department of Biological Sciences, Rutgers University, Newark, NJ 07102

[*]e-mail: ckalodim@umn.edu

Supplementary Results

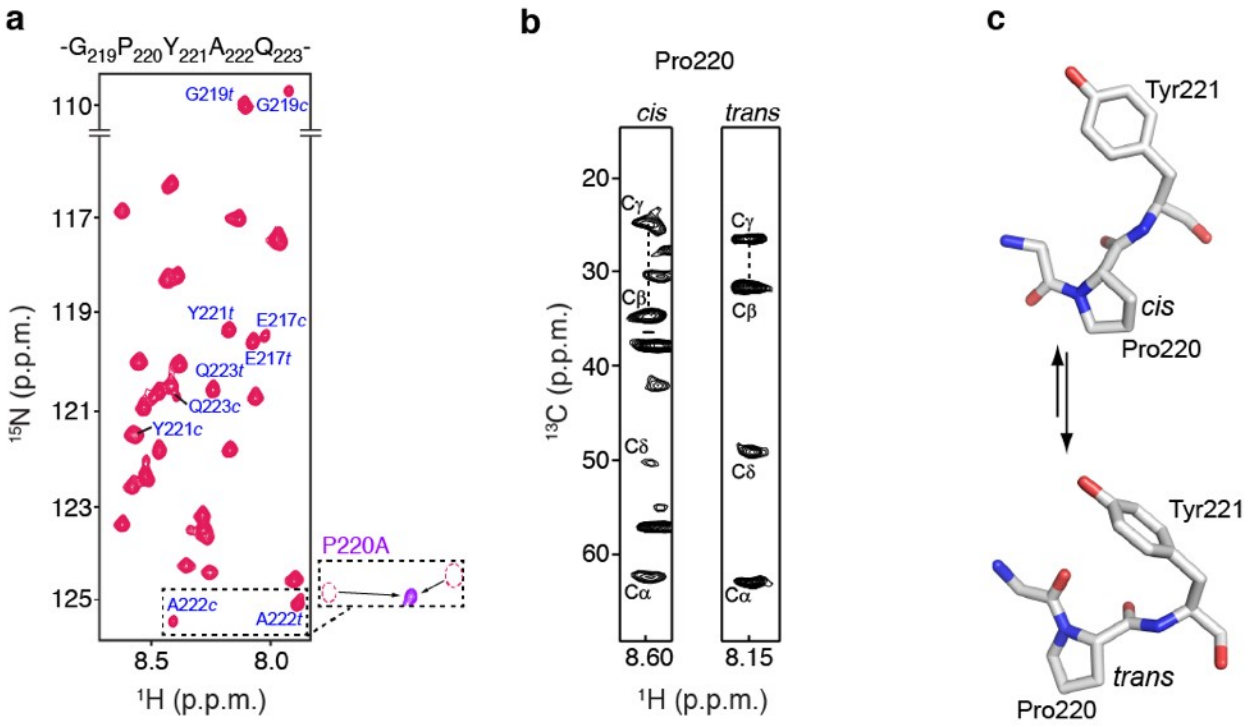

Supplementary Figure 1 | *Cis−trans* isomerization in CrkII. (a) Zoomed view of the ^{1}H-^{15}N heteronuclear single quantum coherence (HSQC) NMR spectrum of a CrkII construct encompassing the sequence around Pro220. The P220A mutant adopts one unique conformation in contrast to the two conformations of wild-type CrkII. Volume integration of cross peaks corresponding to the two conformations indicate that the *trans:cis* population ratio is 3:1 at room temperature. The effect of Pro220 *cis−trans* isomerization is local, with only 7 residues (Glu217-Gln223) showing duplicate peaks. This is expected since Pro220 is located in an unstructured region of the linker. The P220A mutation (magenta) abolishes the heterogeneity. The spectrum of full length human CrkII is shown in Fig. 1b. **(b)** Strips from the CCO-NH spectra showing the ^{13}C chemical shift of Pro220 carbon skeleton. The difference in chemical shift between the $^{13}C_{\beta}$ and the $^{13}C_{\gamma}$ for the two conformations of Pro220 provides evidence for the existence of *cis* and *trans* conformations of the Gly219−Pro220 bond. **(c)** Local structural changes as a result of the *cis−trans* isomerization about the Gly219−Pro220 prolyl bond. The structure of the *cis* and *trans* isomers of the Gly219−Pro220 moiety is shown.

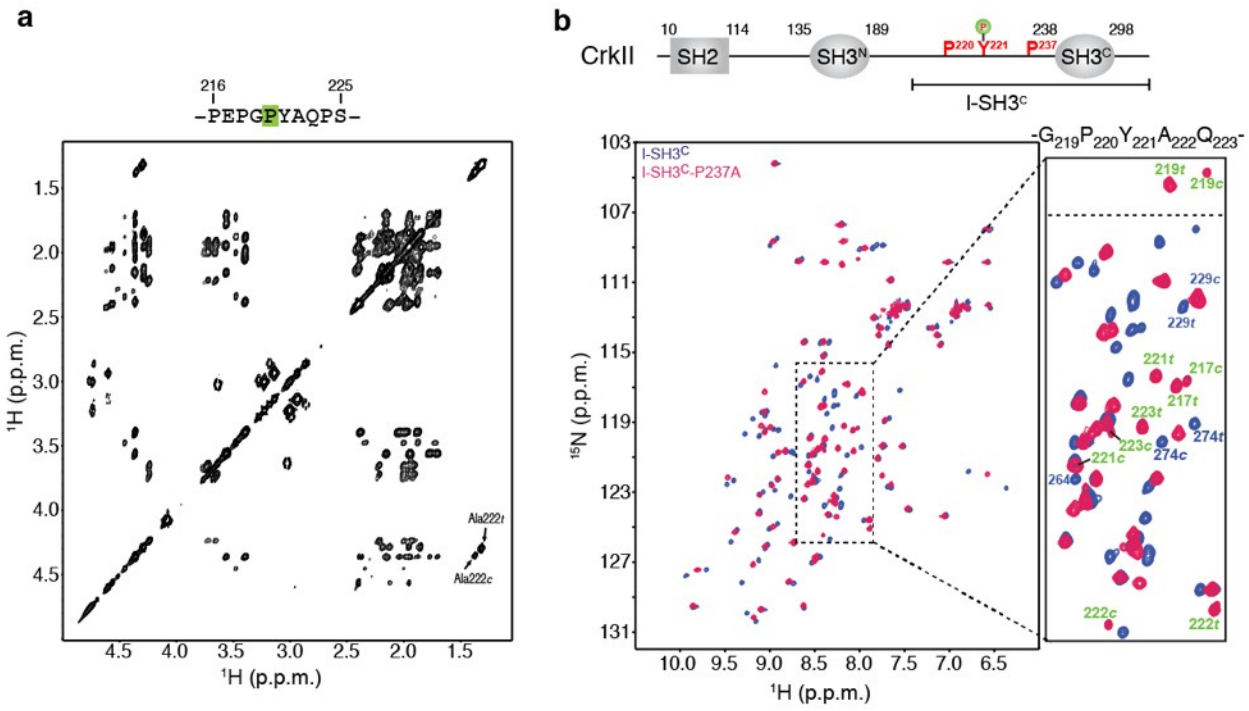

Supplementary Figure 2 | Only Pro220 undergoes *cis*−*trans* isomerization in human CrkII. (a) ^{1}H-^{1}H 2D ROESY spectrum of a peptide consisting of residues Pro216-Pro225 shows that the isomerization process at Pro220 is an intrinsic property of this sequence. **(b)** The isomerization process at Pro220 is distinct from, and independent of, the isomerization process at Pro237 (human CrkII numbering) previously identified in CrkII from chicken[1,2]. Substitution of Pro237 by Ala in CrkII from chicken abolishes the Pro237 isomerization but has no effect on the Pro220 isomerization, as shown in the ^{1}H-^{15}N HSQC spectra. The isomerization process at Pro237 is species-specific and while is present in chicken our NMR analysis indicates that is not present in human CrkII, in agreement with recently published biophysical data[3].

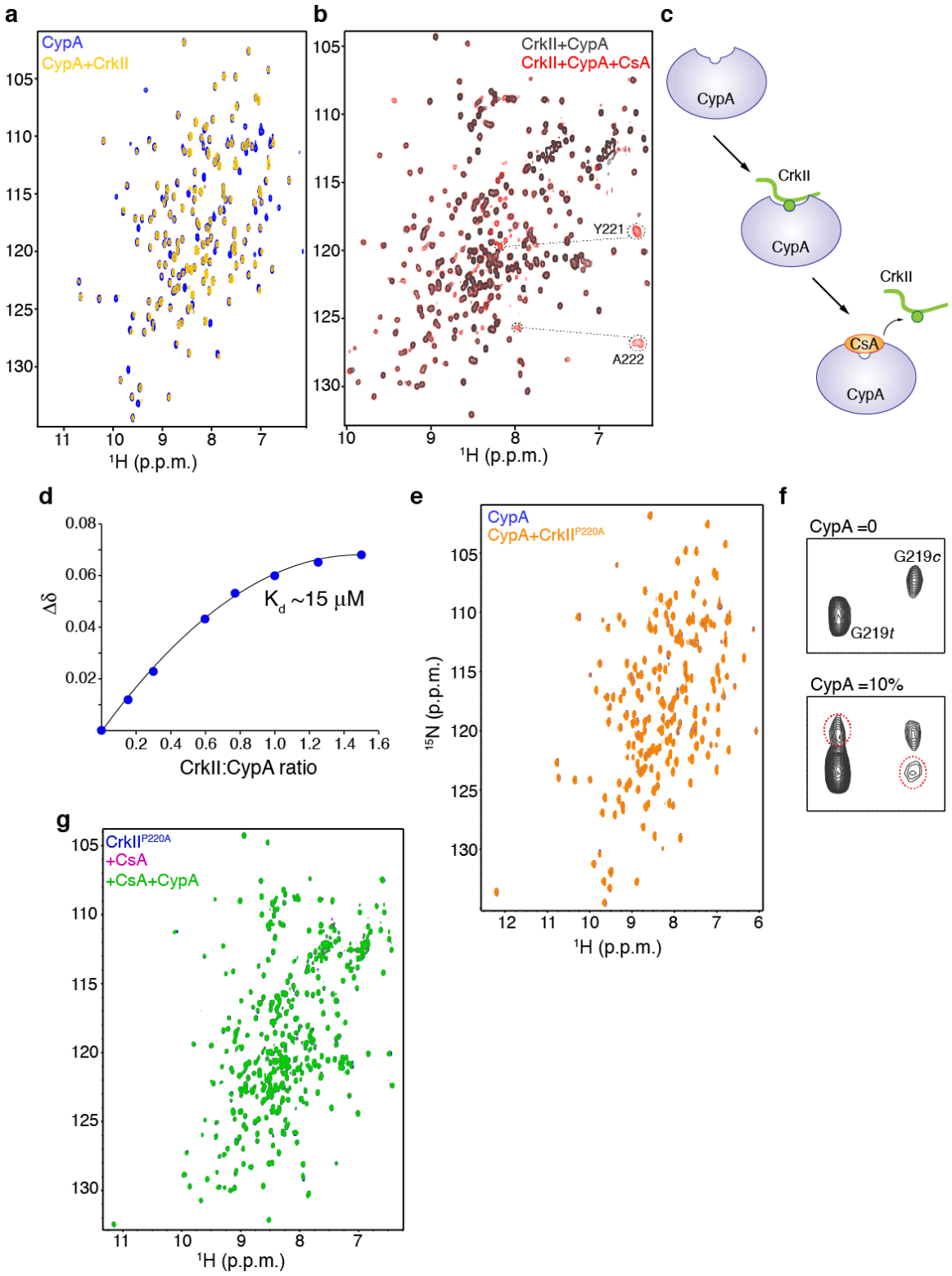

Supplementary Figure 3 | Interaction between CypA and CrkII monitored by NMR. (a) Overlaid ^{1}H-^{15}N HSQC NMR spectra of labeled CypA (blue) and equimolar unlabeled CrkII (yellow). **(b)** Overlaid ^{1}H-^{15}N HSQC NMR spectra of ^{15}N labeled CrkII in complex with unlabeled CypA (grey) and in the presence of CsA (red). CsA displaces CrkII from the binding site on CypA as indicated by the appearance of the CrkII resonances (e.g. Tyr221 and Ala222 zoomed inside the circles on the right) whose intensity is near zero in

the complex of CrkII with CypA. **(c)** Schematic showing the competition between CrkII and CsA for the catalytic site of CypA. **(d)** Representative binding isotherm of the titration of CrkII to ^{15}N-labeled CypA monitored by NMR. $\Delta\delta$ is the composite chemical shift change upon binding. The K_d value (15±4 μM) was calculated and averaged using four residues (Ser99, Ala101, Asn102 and Gln111). The CypA concentration was ~300 μM. **(e)** Overlaid ^{1}H-^{15}N HSQC NMR spectra of labeled CypA (blue) and equimolar unlabeled CrkII^{P220A} (orange) showing that the CrkII^{P220A} mutation abrogates binding to CypA. **(f)** Expansion of 2D ^{1}H-^{15}N ZZ-heteronuclear exchange NMR spectra of ^{15}N-labeled CrkII in the absence and presence of catalytic amounts of CypA. The exchange peaks are denoted by the red dotted circles. The amide resonances corresponding to the *cis* and *trans* isomers of Gly219 residues are shown. **(g)** Overlaid ^{1}H-^{15}N HSQC NMR spectra of labeled CrkII^{P220A} (blue), equimolar CsA (magenta) and equimolar CypA (green) showing that CrkII^{P220A} does not interact with CsA or CypA.

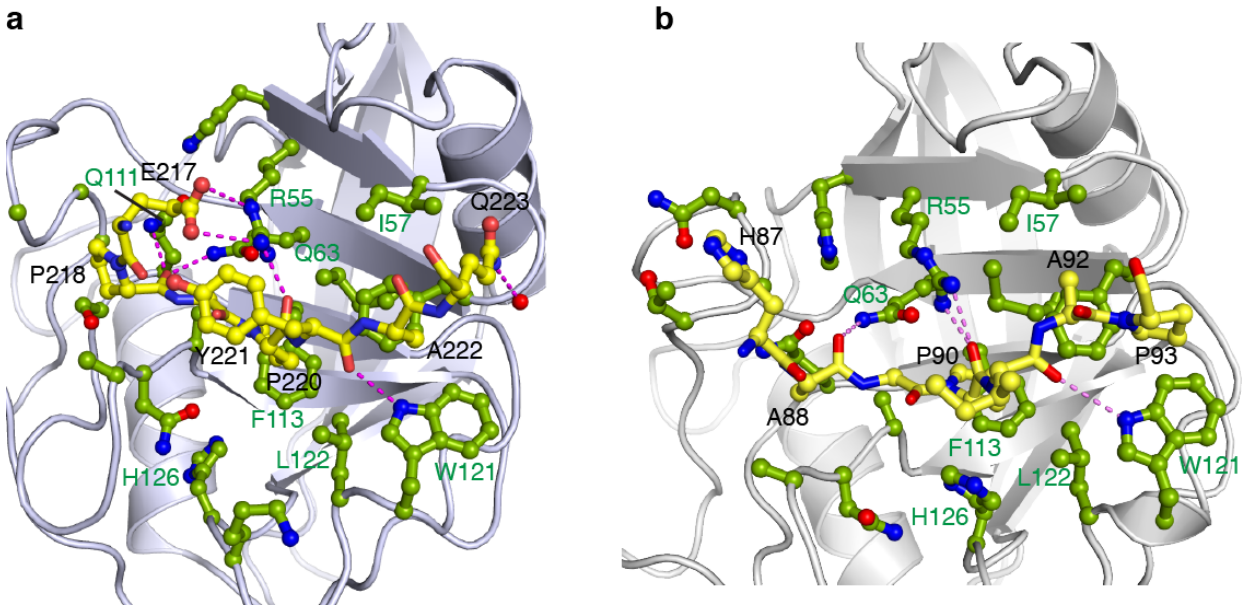

Supplementary Figure 4 | CypA binding mode to substrates. Structure comparison of CypA in complex with **(a)** CrkII (present work, PDB ID 2MS4) and **(b)** HIV-A CA (PDB ID 1M9C). Magenta dotted lines denote polar contacts (hydrogen bond and/or salt bridges).

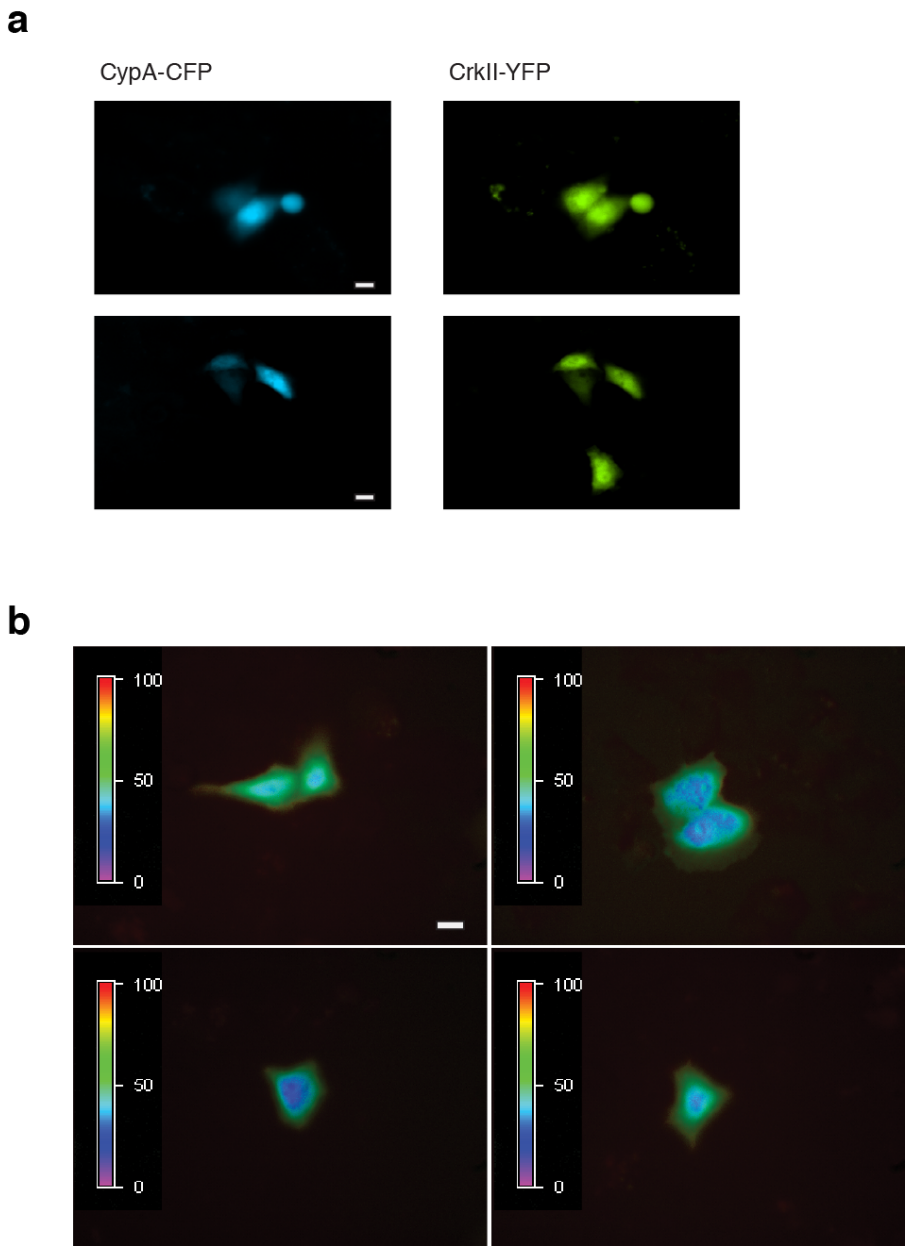

Supplementary Figure 5 | FRET study of CypA-CrkII complex formation in cytoplasm. (a) HeLa cells transiently co-transfected with plasmids containing CypA-CFP and CrkII-YFP showing expression of CypA-CFP and CrkII-YFP. **(b)** FRET analysis of HeLa cells transiently co-transfected with CypA-CFP and CrkII-YFP. The FRET efficiency (%) is color coded in the left bar from 0-100. Cells were imaged 24 hours after transfection. The FRET efficiency calculated for 6 cells show an average of 70 ±3.3%. Scale bars: 20 μm.

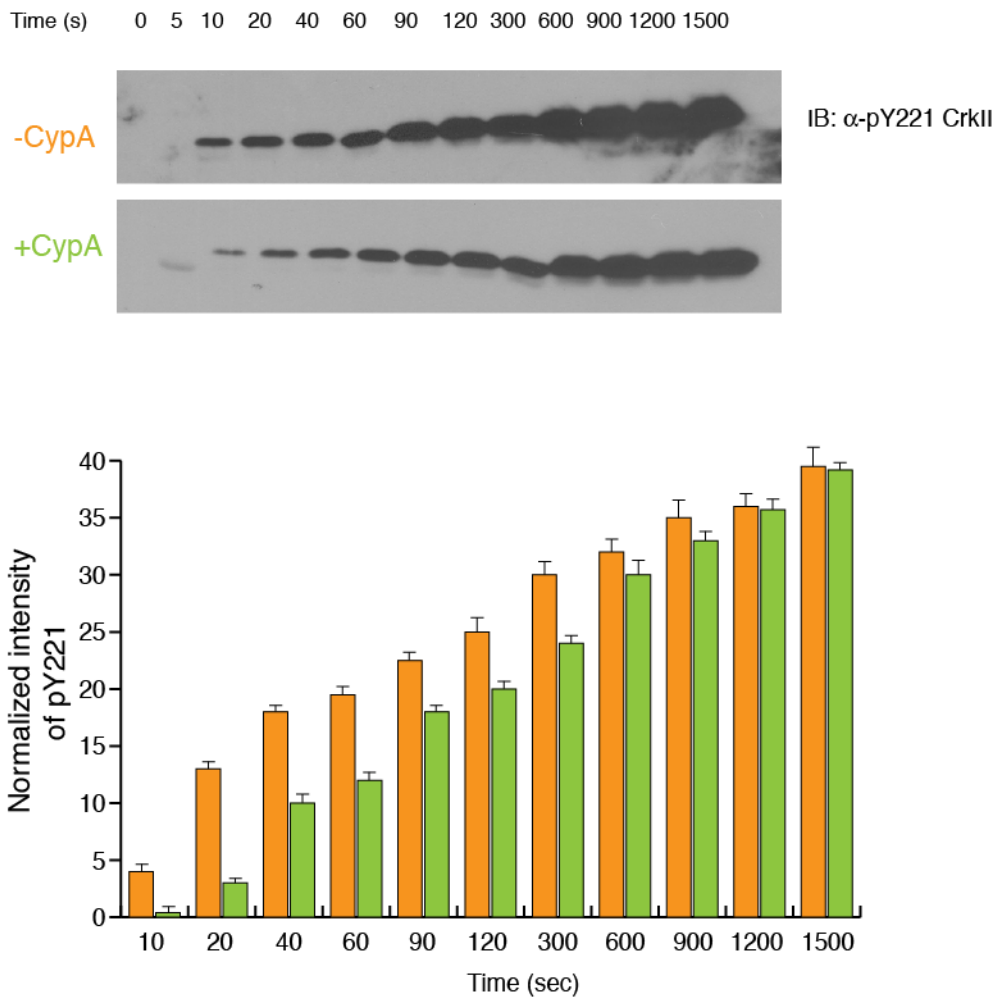

Supplementary Figure 6 | Effect of CypA binding on CrkII Tyr221 phosphorylation. In vitro kinase assay of CrkII with Abl kinase in the presence and absence of CypA was analyzed by SDS-PAGE and western blotting with anti-CrkII pTyr221 antibody (top). The gel shown is a representative of 3 independent experiments. The intensity of the bands were quantified and plotted (bottom). Without CypA (orange) and with CypA (green) (±SEM).

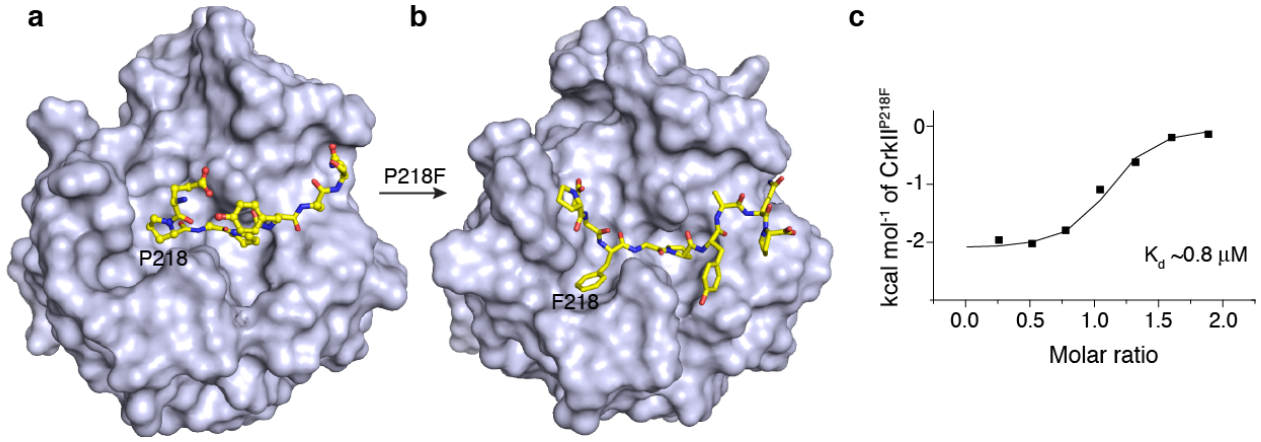

Supplementary Figure 7 | Increasing the affinity of the CrkII-CypA complex. (a) Structure of the CypA–CrkII complex and **(b)** structural model of the CypA–CrkIIP218F complex. Pro218 mutation to Phe (CrkIIP218F mutant) gives rise to optimized inter-molecular binding interface. The hydrophobic pocket of CypA that interacts with CrkII Phe218 is unoccupied in the complex with the wild type CrkII. **(c)** ITC data showed that CrkIIP218F binds to CypA with an improved affinity (K_d ~0.8±0.3 µM) by a factor of ~20 compared to wild type CrkII. Protein samples were extensively dialyzed against the ITC buffer containing 50 mM KPi, pH 6.8, 150 mM NaCl and 1 mM TCEP at 8 ºC.

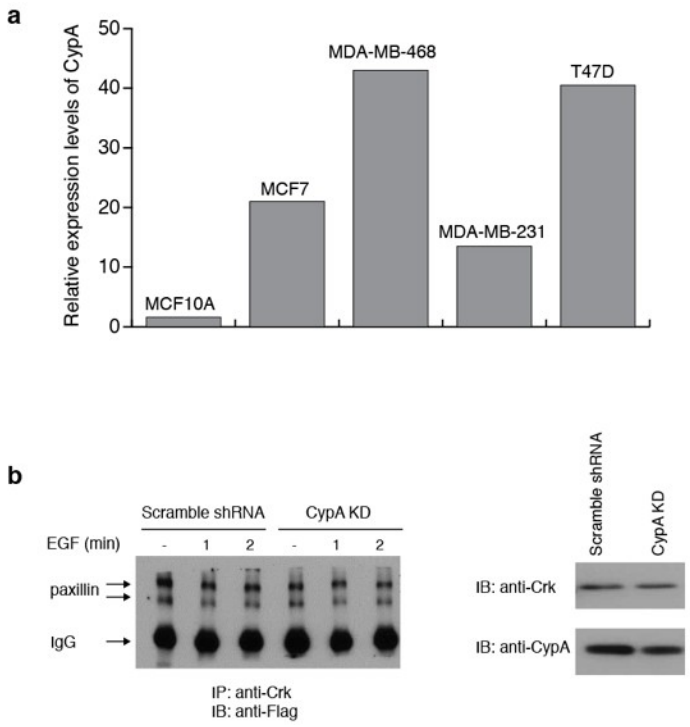

Supplementary Figure 8 | Expression of CypA in various cancer cell lines. (a) Lysates of MCF10A, a non-transformed human mammary epithelial cell line, and human breast cancer cell lines MCF7, MDA-MB-468, MDA-MB-231 and T47D, were analyzed by western blotting with anti-CypA and anti-actin antibodies. Shown is quantification of CypA expression levels normalized to beta-actin for each sample represented as fold increase over MCF10A. **(b)** MDA-MB-468 cells stably expressing scrambled or CypA shRNA were maintained in culture until CypA expression levels were partially restored. The experiment in Fig. 4c was performed on these cells. Western blotting of cell lysate with anti-flag (left) show comparable association of CrkII and paxillin both in the cells treated with scrambled or CypA shRNA. Anti-CypA and anti-CrkII blots (right) show restoration of CypA expression.

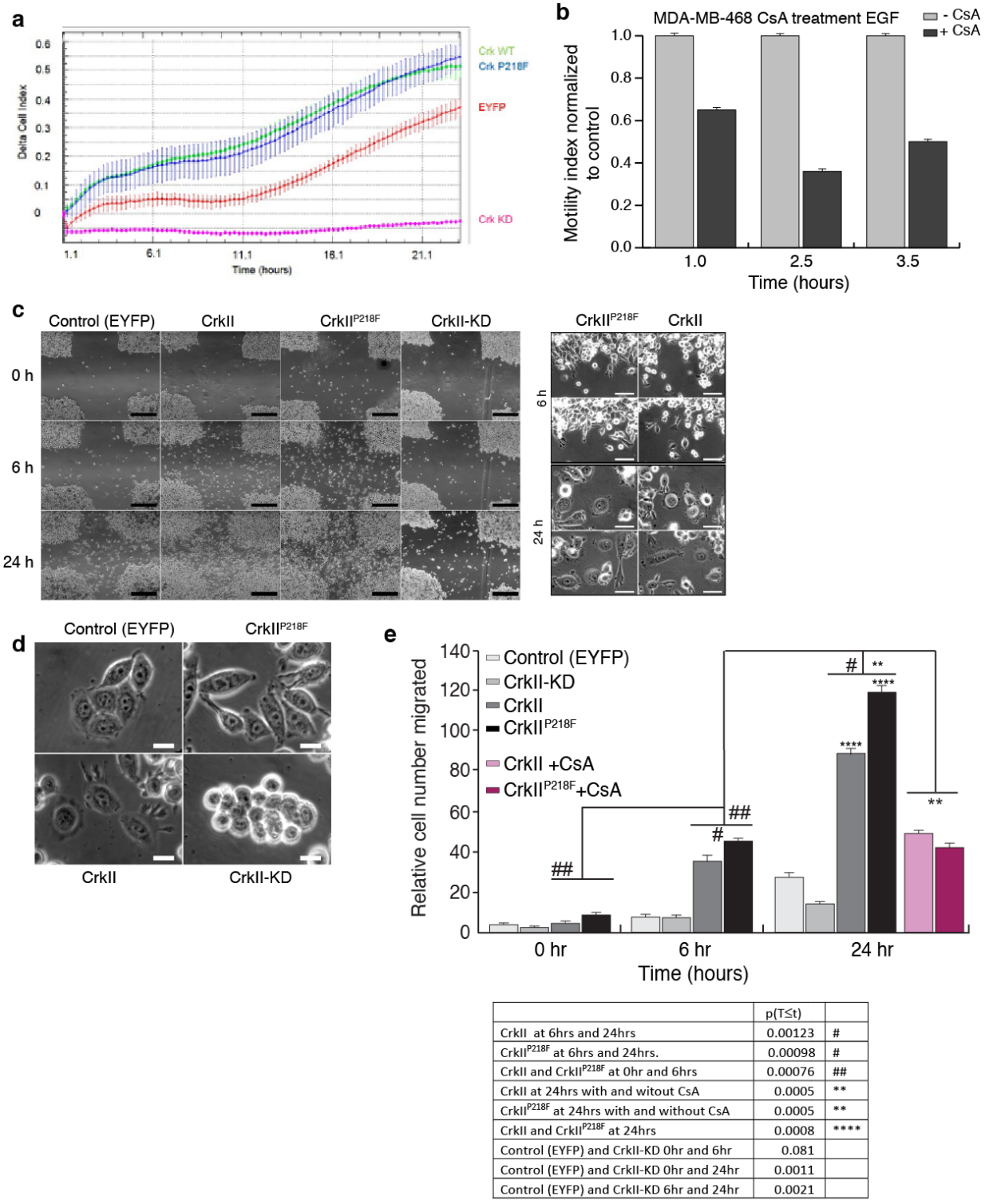

	p(T≤t)	
CrkII at 6hrs and 24hrs	0.00123	#
CrkII^{P218F} at 6hrs and 24hrs.	0.00098	#
CrkII and CrkII^{P218F} at 0hr and 6hrs	0.00076	##
CrkII at 24hrs with and witout CsA	0.0005	**
CrkII^{P218F} at 24hrs with and without CsA	0.0005	**
CrkII and CrkII^{P218F} at 24hrs	0.0008	****
Control (EYFP) and CrkII-KD 0hr and 6hr	0.081	
Control (EYFP) and CrkII-KD 0hr and 24hr	0.0011	
Control (EYFP) and CrkII-KD 6hr and 24hr	0.0021	

Supplementary Figure 9 | Effect of the CypA-CrkII complex on cell migration. (a) Cell motility of MDA-MB-468 cells was monitored and analyzed towards EGF (25 ng ml^{-1}) in real-time using xCelligence technology (Roche). The cells stably express the indicated protein (EYFP, CrkII, or CrkII^{P281F}). Delta cell index is plotted on the y-axis as an average of duplicate samples versus time on the x-axis. Cell index was recorded every 15 minutes. **(b)** MDA-MB-468 cells were serum-starved, pre-treated with CsA (15 μM) for 30 minutes and then motility of cells was analyzed towards EGF in real-time using xCelligence technology (Roche). Cell Index is plotted on the y-axis after background subtraction and normalization to

control. Without CsA(light grey) and with CsA (dark grey) **(c)** Wound healing assay. Cells were cultured to near confluence, scratched using a pipette and imaged after immediately scratching (0 hours) followed by 6 and 24 hours. The magnified images for the respective cell lines clearly show the extensive lamellipodia formed by the overexpression of CrkII and CrkII^{P218F}. The control cells and the CrkII-KD do not display such structures. Scale bars: 500 μm (left panel), 50 μm (right panel). **(d)** The magnified images for the respective cell lines clearly show the extensive lamellipodia formed by the overexpression of CrkII and CrkII^{P218F}.The control cells and the CrkII-KD do not display such structures. Scale bars: 20 μm. **(e)** Summary of the measurement of cell migration from the wound healing assay in Fig. 5b and supplementary Fig. 9c was quantified for each condition indicated. Data represent mean ±SEM. Two tailed t-test was performed for samples indicated.

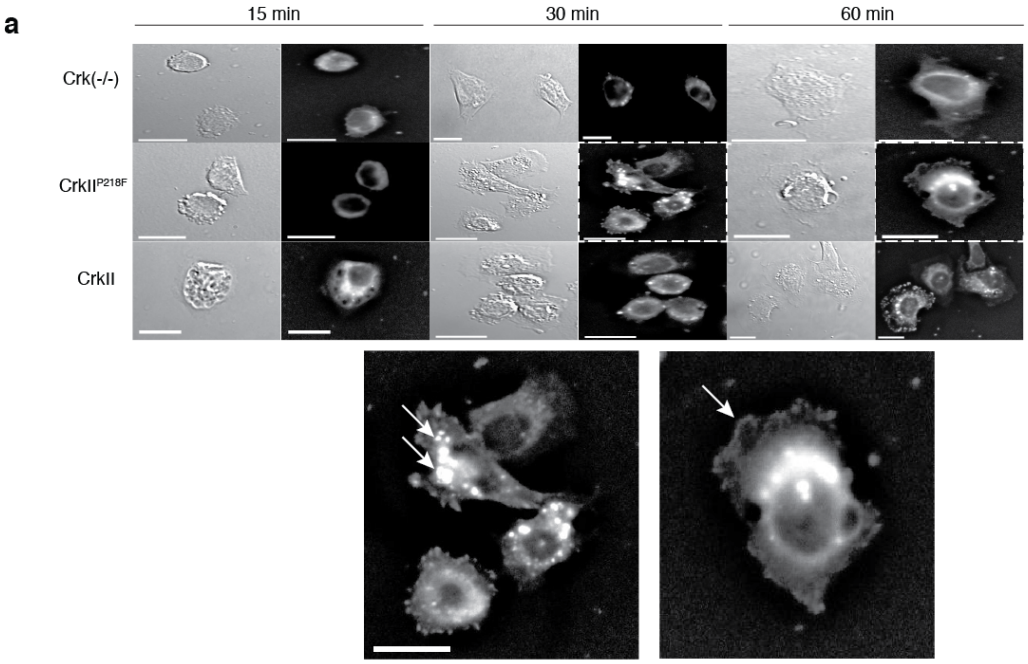

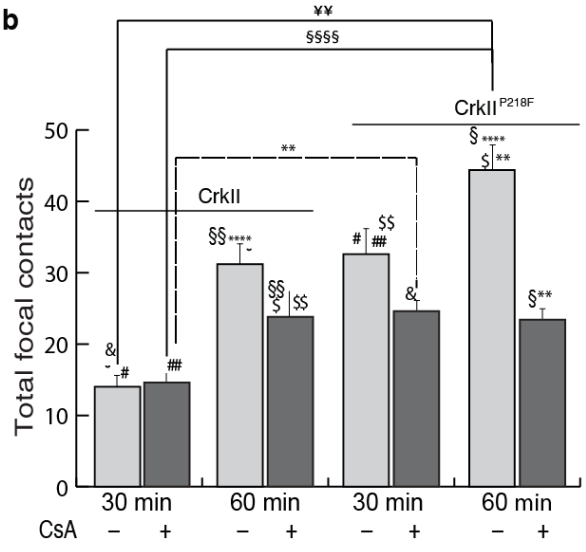

a. CrkII 30 mins without CsA
b. CrkII 30mins with CsA
c. CrkII 60mins without CsA
d. CrkII 60 mins with CsA
e. CrkII P218F 30mins without CsA
f. CrkII P218F 30mins with CsA
g. CrkII P218F 60mins without CsA
h. CrkII P218F 60mins with CsA

	P(T<=t)	
b and g	0.0000007	§§§§
a and g	0.000002	¥¥
f and g	0.00004	¥¥
b and f	0.0004	**
g and h	0.0004	**
d and g	0.0007	$
b and e	0.0008	$$
a and e	0.001	&
b and c	0.001	##
a and c	0.001	˘
a and e	0.001	#
c and g	0.009	****
a and h	0.02	
b and d	0.02	
e and g	0.02	
b and h	0.022	
a and d	0.03	
e and f	0.055	
e and h	0.06	
d and e	0.09	
c and f	0.109	
c and h	0.12	
c and d	0.15	
c and e	0.716	
f and h	0.729	
a and b	0.755	
d and f	0.833	
d and h	0.931	

Supplementary Figure 10 | Focal contact quantification by fluorescent microscopy and statistical analysis. (a) Panel displaying CrkII (-/-) MEFs or expressing either CrkII or CrkII^{P218F} transiently transfected with GFP-paxillin were seeded and fixed at time points indicated. Cells were imaged with a Plan-Apo 63X oil immersion objective on an inverted wide field Zeiss microscope using Axiovision

software. Deconvolution was iterative with autolinear normalization for all images. Scale bar: 20 μm **(b)** Focal contacts based on signal from GFP-Paxillin (panel a) were quantified for each cell line and treatment using ImageJ and plotted. Results shown are an average of six cells per treatment. Error bars represent mean ±SEM (n=6; two-tailed t-test). Significance values are sorted from most significant (top) to least significant (bottom). Data sets displaying $p < 0.01$ are indicated on the figure with the respective symbols.

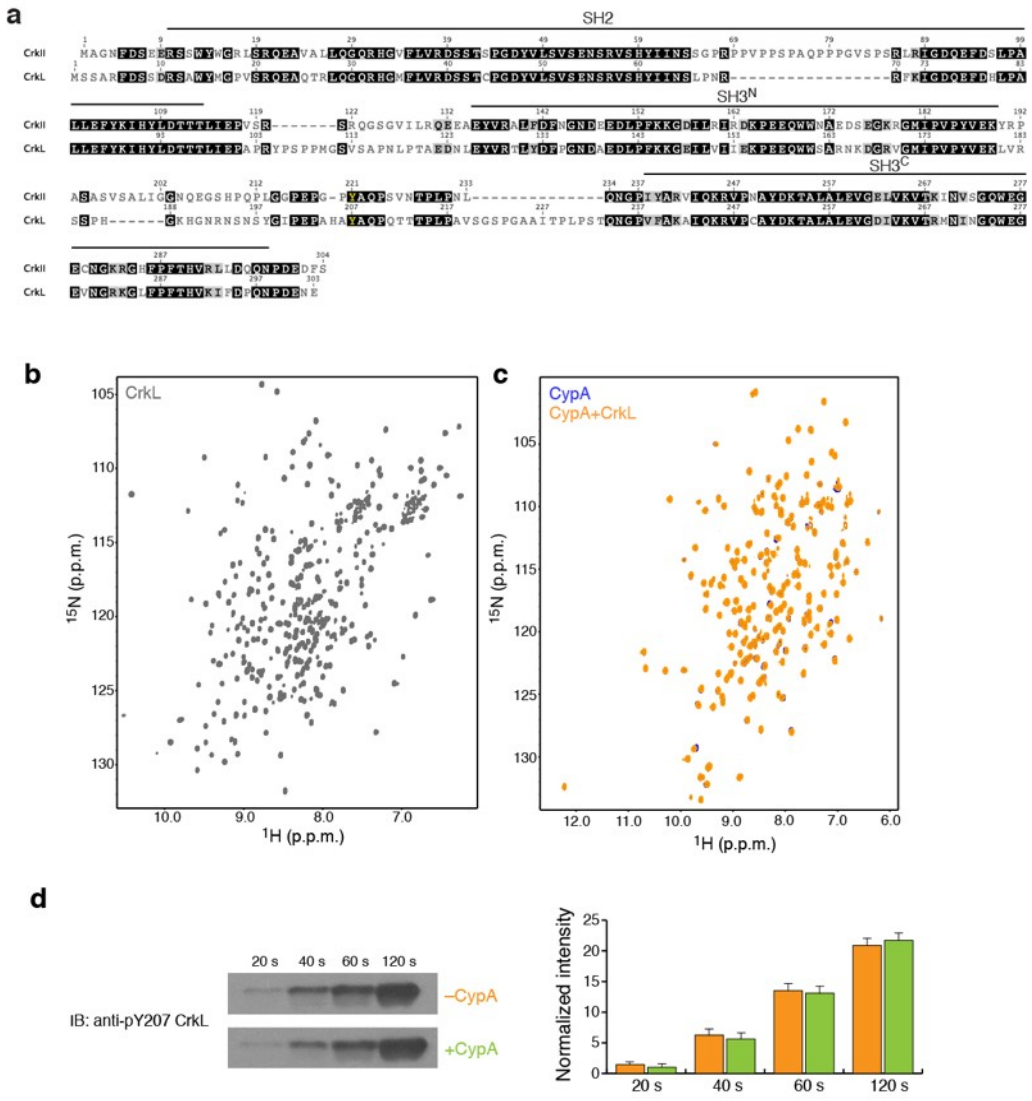

Supplementary Figure 11 | CrkL does not interact with CypA. (a) Sequence alignment of human CrkII and CrkL. **(b)** ^{1}H-^{15}N HSQC NMR spectra of CrkL. No *cis*−*trans* isomerization was observed. **(c)** Overlaid ^{1}H-^{15}N HSQC NMR spectra of ^{15}N labeled CypA in the absence (blue) and presence of equimolar unlabeled CrkL. No interaction was observed. **(d)** In vitro kinase assay of CrkL with Abl kinase in the presence (bottom) and absence (top) of CypA was analyzed by SDS-PAGE and western blotting with anti-CrkII pY207 antibody (left). The intensity of the bands were quantified and plotted (right) Without CypA (orange) and with CypA (green). CypA has no effect on CrkL Tyr207 phosphorylation since, in contrast to CrkII, CrkL does not interact with CypA.

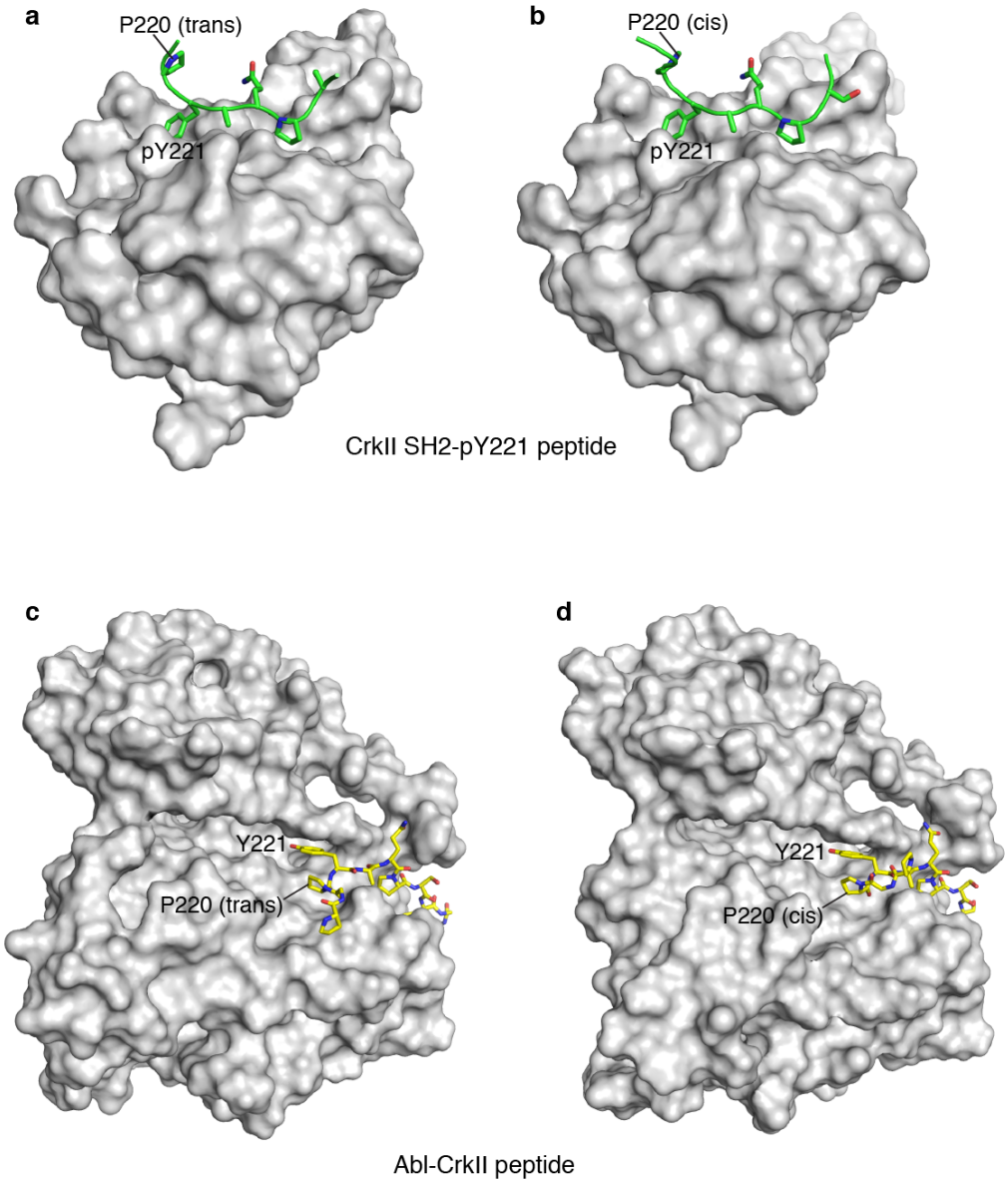

Supplementary Figure 12 | Structure modeling of the interaction of the CrkII peptide with the CrkII SH2 and the Abl kinase. The structure of the phosphorylated CrkII pY221 peptide in complex with the SH2 domain of CrkII with Pro220 in the *trans* (PDB ID 1JU5) **(a)** and in the *cis* (modeled) **(b)** conformation. The structures show that Pro220 makes no contacts with the SH2 domain and thus the presence of either the trans or cis conformer does not affect complex formation. The structure of the CrkII peptide in complex with the Abl kinase where Pro220 is in the *trans* **(c)** and the *cis* **(d)** conformation. Both conformers were modeled using the structure of Abl with a substrate (PDB ID 2G1T) and the structure of the insulin receptor kinase in complex with a substrate (PDB ID 1IRE). The structures show that the CrkII peptide juxtaposes with the active site of Abl equally well in either conformer corroborating our NMR data showing that both conformers get phosphorylated by Abl.

Fig. 3a

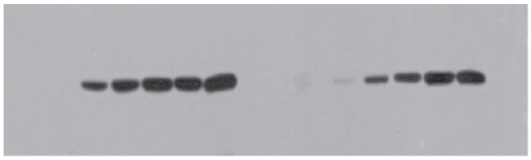

Fig. 3b Abl Blot

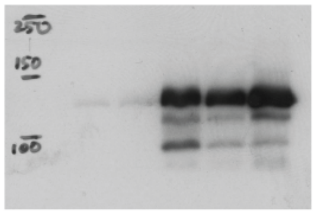

Fig. 3b pY221 CrkII Blot

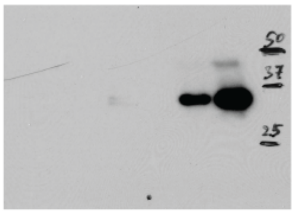

Fig. 3b CypA Blot

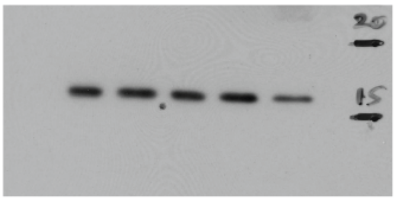

Fig. 3c CrkII blot

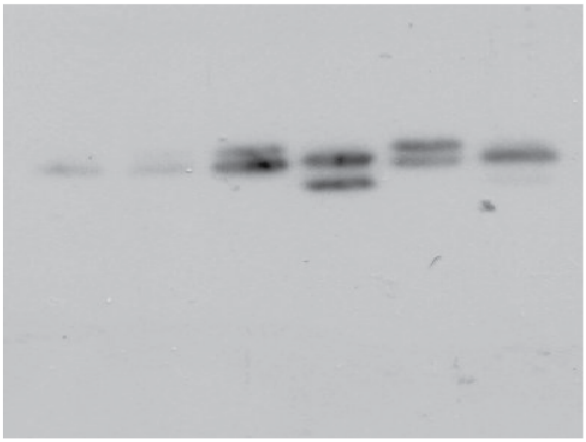

Fig. 3c CrkII pY221 blot

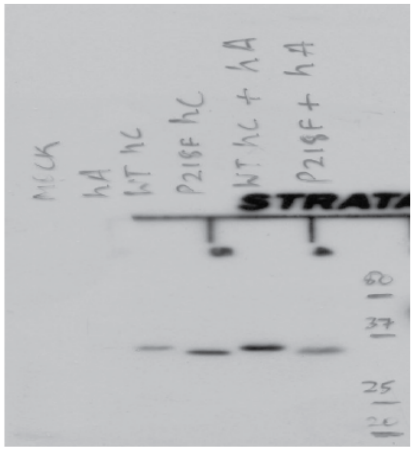

Fig. 4a CrkII pY221 blot

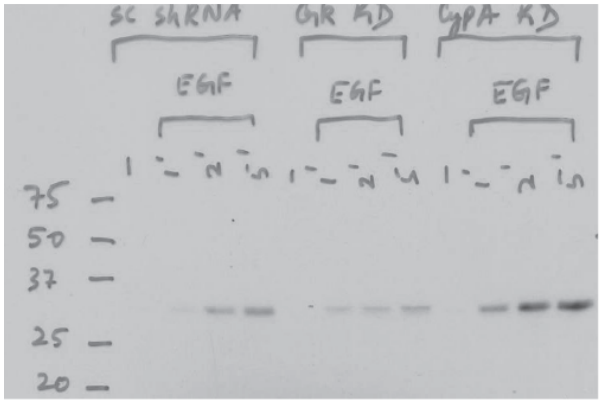

FIg. 4a CrkII blot

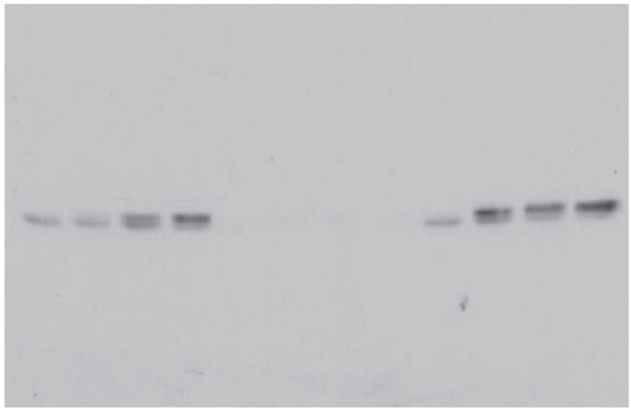

Fig. 4a CypA blot

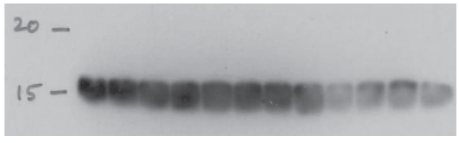

Fig. 4b pY221 Blot

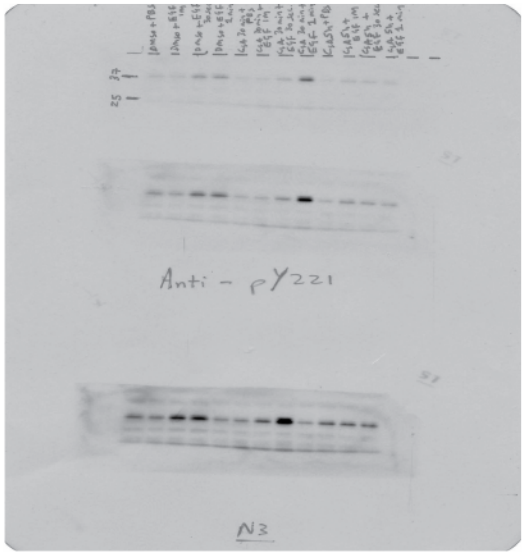

Fig. 4b CrkII Blot

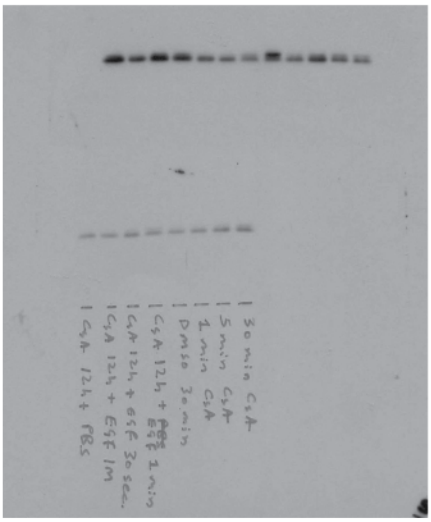

Fig. 4b Actin Blot

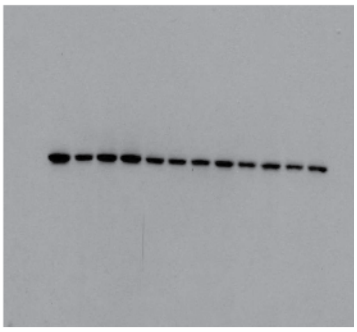

Fig. 4b pY Blot

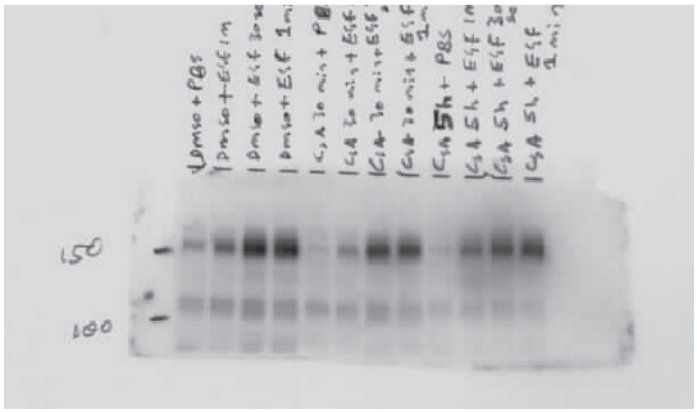

Fig. 4c Blot

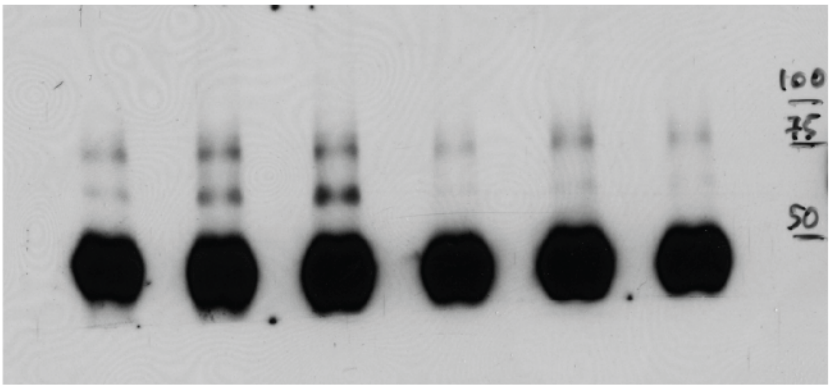

Supplementary Fig. 6

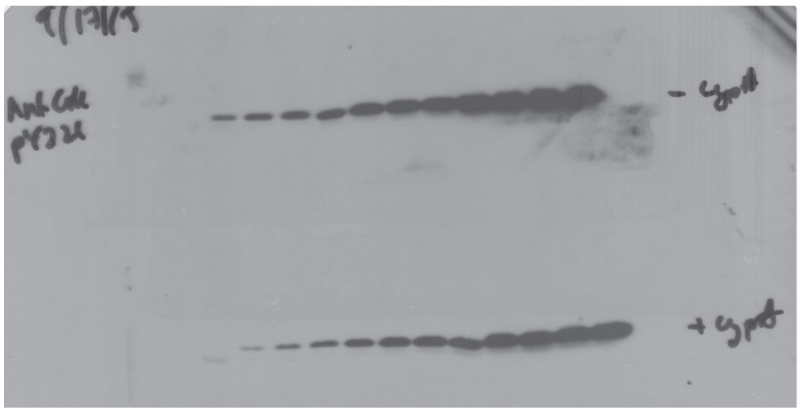

Supplementary Fig. 8b

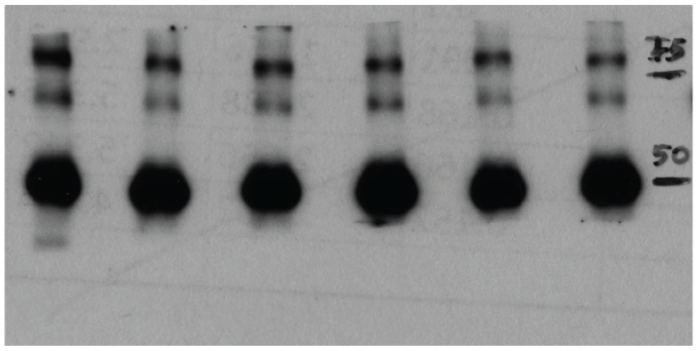

Supplementary Fig. 11

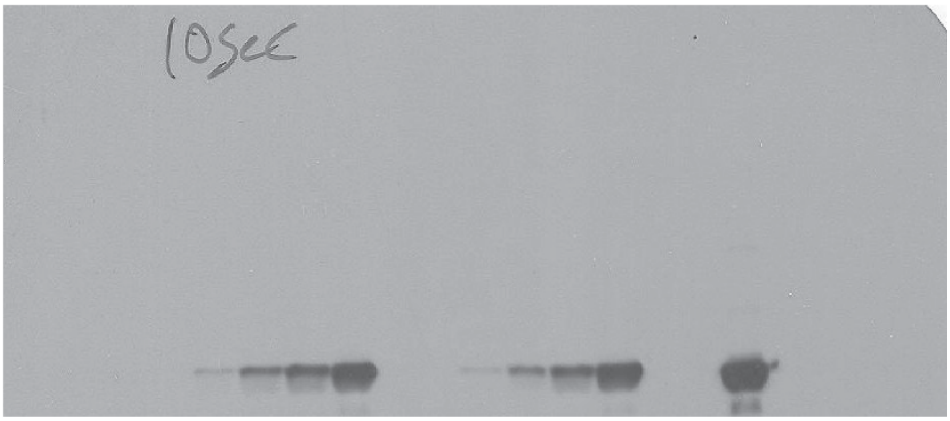

Supplementary Figure 13 | Full-size western blot gels related to the indicated Figures.

Supplementary Table 1 | Summary of NMR structural statistics of the CypA−CrkII complex

	Protein
NMR distance and dihedral constraints	
Distance constraints	
Total NOE	2114
Intra-residue	424
Inter-residue	
Sequential ($\|i-j\|=1$)	557
Medium-range ($\|i-j\|<4$)	285
Long-range ($\|i-j\|>5$)	853
Intermolecular	12
Hydrogen bonds	125
Total dihedral angle restraints	368
ϕ	126
ψ	132
Structure statistics	
Violations (mean and s.d.)	
Distance constraints (Å)	0.0014(0.013)
Dihedral angle constraints (º)	0.32(1.04)
Max. dihedral angle violation (º)	12.1
Max. distance constraint violation (Å)	0.3
Deviations from idealized geometry	
Bond lengths (Å)	0.018
Bond angles (º)	1.2
Impropers (º)	2.0
Average pairwise r.m.s. deviation** (Å)	
Heavy	0.82
Backbone	0.50

**Structural statistics were computed for the ensemble of 20 deposited structures (PDB ID: 2MS4)

References

1. Sarkar, P., Reichman, C., Saleh, T., Birge, R.B. & Kalodimos, C.G. Proline cis-trans isomerization controls autoinhibition of a signaling protein. Molecular Cell 25, 413-426 (2007).

2. Sarkar, P., Saleh, T., Tzeng, S.-R., Birge, R.B. & Kalodimos, C.G. Structural basis for regulation of the Crk signaling protein by a proline switch. Nature Chemical Biology 7, 51-57 (2011).

3. Schmidpeter, P.A. & Schmid, F.X. Molecular determinants of a regulatory prolyl isomerization in the signal adapter protein c-CrkII. ACS Chem Biol 9, 1145-52 (2014).